Int. J. Heat Mass Transfer. Vol. 17, pp. 595–607. Pergamon Press 1974. Printed in Great Britain

EFFECTS OF HOLE GEOMETRY AND DENSITY ON THREE-DIMENSIONAL FILM COOLING

R. J. GOLDSTEIN and E. R. G. ECKERT
Heat Transfer Laboratory, Mechanical Engineering Department, University of Minnesota, Minneapolis, Minnesota 55455, U.S.A.

and

F. BURGGRAF†
Aircraft Gas Turbine Division, General Electric Company, Cincinnati, Ohio 45215, U.S.A.

(*Received* 4 *October* 1972 *and in revised form* 22 *March* 1973)

Abstract—Film cooling downstream of secondary gas injection through discrete holes has been studied experimentally. The influences of hole geometry, secondary fluid density, and mainstream boundary layer thickness are described. Significant improvements in the film cooling effectiveness are observed by having the coolant passages widened before the exit of the secondary fluid. The use of a relatively dense secondary fluid, as might be encountered in many applications, requires a significantly higher blowing rate to cause jet separation from the surface than when the densities of the freestream and secondary stream are the same. This results in considerably better film cooling over an important range of density ratios.

NOMENCLATURE

D, diameter of cylindrical channel or metering section of shaped hole;

I, momentum flux ratio, $\dfrac{\rho_2 U_2^2}{\rho_\infty U_\infty^2}$;

M, blowing rate, $\rho_2 U_2/\rho_\infty U_\infty$;

R, ratio of hole exit area to hole inlet area. Exit area is defined by the imaginary intersection of the hole with a plane which is perpendicular to the channel axis and located where the axis emerges from the surface;

Re_D, Reynolds number $\dfrac{\rho_\infty U_\infty D}{\mu_\infty}$;

s, area of holes per unit span, i.e. effective slot height. (Metering hole area used for shaped channel);

T, temperature;

U_∞, mainstream velocity;

U_2, average velocity in injection channel. (Metering hole area used for shaped channel);

X, distance downstream of injection hole;

Z, lateral distance from tunnel centerline;

δ^*, boundary layer displacement thickness;

μ, dynamic viscosity;

ρ, density;

η, effectiveness $\dfrac{T_{aw}-T_\infty}{T_2-T_\infty}$;

γ, side spreading angle for each side of shaped hole (10°).

Subscripts

∞, mainstream;

2, secondary or injection stream;

aw, adiabatic wall;

$\mathbb{C}$, downstream of center of injection holes.

1. INTRODUCTION

THERE IS renewed interest in the process of film cooling as a means of protecting solid surfaces exposed to high temperature gas streams. With a two-dimensional flow, the film cooling performance can be predicted relatively well by analysis or by interpolation or extrapolation of previous experimental results. With three-dimensional flow, however, prediction of film cooling is more

† Fred Burggraf passed away in the summer of 1973 while in the full bloom of his technical career. His co-authors join with his fellow workers at General Electric and the Heat Transfer Community at large to express sorrow at our loss. Fred was untiring and inspiring in his work in Heat Transfer, particularly as it applied to the development of the modern gas turbine engine. He will be sorely missed by all who knew him as both friend and colleague.

difficult. This is particularly true when there are relatively sharp discontinuities at the entrance of the secondary flow stream, as occurs if the secondary fluid enters not through a continuous or almost continuous slot or porous section, but is introduced through discrete holes in the surface. Previous studies (e.g. [1]) indicate that for the same flow of secondary fluid, considerably less cooling or protection is obtained with discrete holes than with injection through a continuous slot. This less efficient performance is apparently due to the penetration of the jets from the individual holes into the free stream, permitting the hot free stream gases to flow under the secondary fluid close to the surface to be protected. The intent of the present study is to investigate possible means for improving film cooling effectiveness with injection through discrete holes. To accomplish this, various means were sought which would reduce the penetration of the secondary fluid jet and also increase the lateral spreading of the jets to improve cooling downstream of the region between the injection holes.

A number of studies (cf. [2]) suggest that the trajectory of a three-dimensional jet entering a cross stream is primarily determined by the momentum flux (or dynamic head) ratio of the two fluids, namely $\rho_2 U_2^2/\rho_\infty U_\infty^2$. This may be contrasted to two-dimensional film cooling in which the data can often be correlated using the blowing parameter (mass flux ratio) $\rho_2 U_2/\rho_\infty U_\infty$. The last mentioned parameter is indicative of the enthalpy deficit of the entering secondary fluid and would be expected to play a role in predicting film cooling effectiveness. However, when flow conditions are such that the jet can separate from the surface, the momentum flux ratio cited above can also be of importance. In most previous studies it was not possible to separate the effect of momentum flux ratio, I, from the mass flux ratio, M, as the densities of the fluid streams were approximately equal.

One possible means of keeping the entering jet close to the surface is to give the hole through which the jet leaves the surface a different area and geometry from the metering section, which controls the secondary fluid flow rate. In previous three-dimensional film cooling studies, the metering hole was essentially cylindrical, and the secondary flow channel had a constant circular cross section. In an effort to improve film cooling effectiveness, the geometry near the secondary flow channel exit has been altered in the present study by increasing the exit area. Improved film cooling effectiveness might be expected for two reasons; one is the reduction in momentum flux at the exit of the holes with a decreased penetration of the jet into the free stream. It was also expected that the passageway for the secondary fluid might be designed to produce a Coanda effect at the exit so that injected fluid would follow the surface rather than penetrate into the free stream.

The present study includes film cooling measurements with injection of a secondary gas through discrete holes. Before adiabatic wall measurements were made, flow visualization studies were performed. These visualization studies used a number of different injection channel geometries. Adiabatic wall measurements were then made with two selected flow geometries in a tunnel with an air mainstream. Both air and refrigerant-12 were used as secondary fluids to study the effect of density and the relative importance of the momentum flux and the mass flux ratios. The importance of the mainstream boundary layer thickness was also examined.

II. APPARATUS

Wind tunnel

Adiabatic wall temperature measurements are taken in the 25 cm wide by 13 cm high test section of an open cycle wind tunnel. Air entering the tunnel passes through a filter, a flow straightener, a series of three screens, and a contraction with an area ratio of approximately 9 to 1 before entering the test section. Downstream of the test section are a diffuser and a blower.

The insulated test surface is constructed of Benelex (pressed wood) and is instrumented with a row of 31 thermocouples down its centerline. Several thermocouples are also located off centerline to check for symmetry. Heated jets of secondary air enter through the test surface just upstream of the test surface. A separate plate is provided in which the holes for these jets are drilled. It measures 24 cm by 8 cm (in flow direction) on the test surface and sits on a 1 cm step around its edges, so that the lower surface of this plate measures 22 cm by 6 cm.

The secondary flow system that provides the heated air for the jet consists of a blower, an orifice to meter the flow, an electric heater and a plenum chamber that adjoins the test plate containing the injection holes. The mass flow rate of this system is controlled by a bleed line and valve at the outlet of the blower. Note that the mainstream air is essentially at room temperature while the secondary gas is heated. For the refrigerant-12 injection, the blower was replaced by a pressure regulated supply.

The velocity of the mainflow in the test section is varied from 20 to 55 m/s. The boundary layer on the test surface is "tripped" by a wire at the outlet of the contraction section to ensure that it is both turbulent and uniform across the width of the test section. In the absence of secondary flow, the boundary layer displacement thickness at the point of injection is

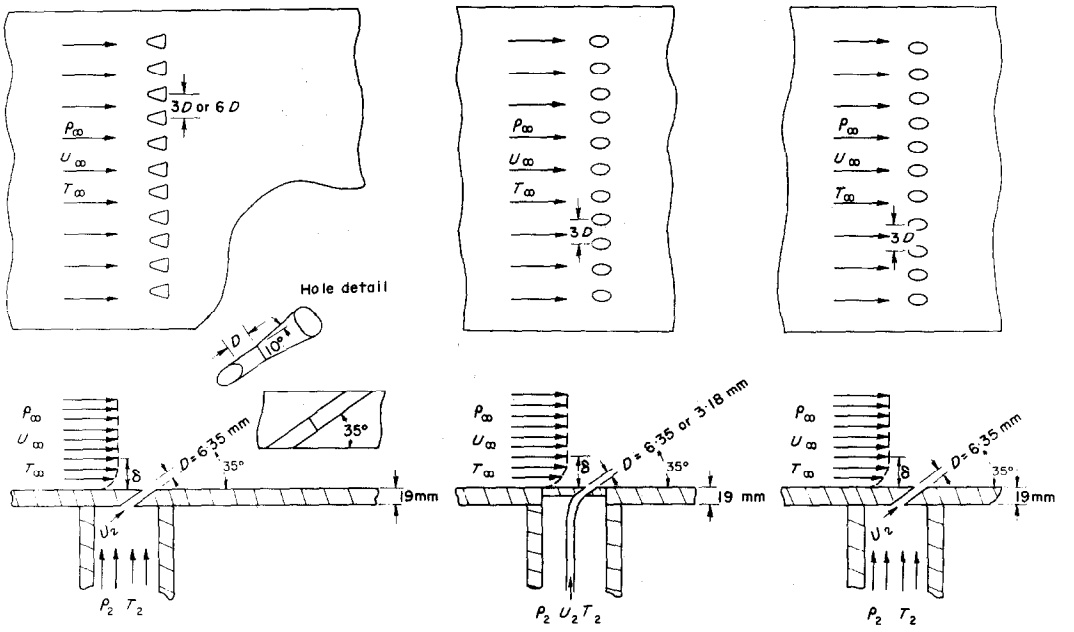

FIG. 1. Geometry of injection section. (a) Shaped injection channels; (b) Long cylindrical injection channels; (c) Cylindrical injection channels through a thin wall.

given by the following empirical relation:

$$\delta^* = 2{\cdot}16\, U_\infty^{-0{\cdot}2}$$

where δ^* is in mm and U_∞ is in m/s.

In addition to the thermocouples in the test wall, a rake of 17 thermocouples is used to measure lateral variations in temperature on the text surface. These thermocouples are spaced at approximately 3 mm intervals. The total width of the rake is 50 mm.

Secondary flow passage

Two different secondary flow channel geometries were used in the experiments. Each had its axis inclined at 35 degrees from the test surface. In one, the cross section of the channel that admits secondary flow is circular throughout its length. This is called a cylindrical or straight hole (or channel or passage). The opening of the hole in the test surface is therefore elliptical, the relative size of the major and minor axes being determined by the angle of the circular cylinder to the test surface: 35 degrees in the results reported herein. In the second type of channel, the metering region at the entrance of the secondary flow is circular, but the channel widens out at an angle of 10° near the exit as shown in Fig. 1a. This is a "shaped hole" (or channel or passage). The diameter of the circular section of such a channel was usually 6·35 mm, although in some of the tests injection sections with 3·18 mm passages were used. For the cylindrical channels, two different secondary flow conditions were maintained: long entrance sections in which developed flow was assured (Fig. 1b), and short ones, approximately 19 mm long, constructed by drilling holes through the wall (Fig. 1c). No appreciable differences were observed in the film cooling results for the tests with long or short secondary flow passages. A relatively thin wall section was also used for the passages widened at the exit (shaped channels) and the channels were cut into the wall. In most experiments with a row of holes across the span of the tunnel the center-to-center spacing of the holes was three diameters (based on circular sections of the hole). A few measurements were taken with secondary injection through a single (straight or shaped) hole.

Flow visualization

A fog of carbon dioxide and water vapor is used in the flow visualization experiments. This fog is generated by placing dry ice and warm water in a pressure vessel. The resulting flow passes through a hose into a plenum chamber and through the flow channel that is being tested. The jet is photographed at the outlet of the hole. The test hole is machined in a section of Plexiglas that can be mounted on one end of the plenum chamber. The diameter of the metering hole is typically 6·4 mm and the Plexiglas is usually 19 mm thick.

The flow visualization studies were made with either the straight holes or the holes shaped as in Fig. 1a. In all cases a single hole was used. At times a fan was used to provide some indication of the influence of a free stream.

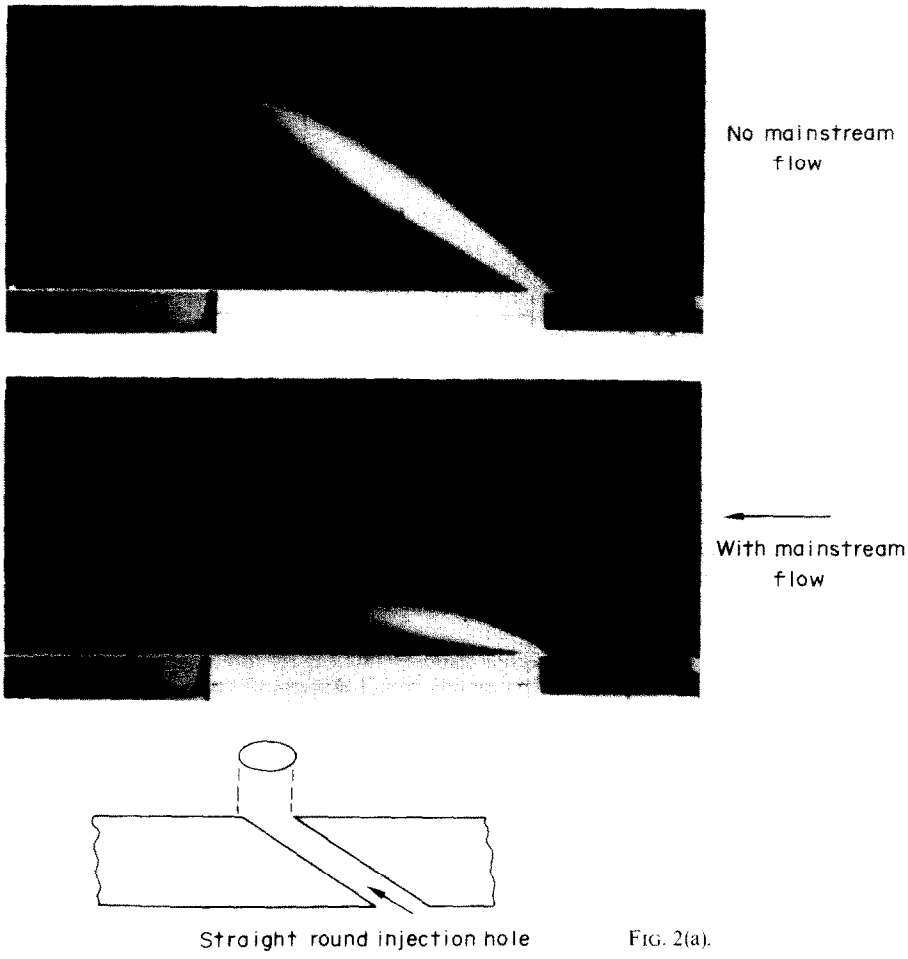

FIG. 2(a).

III. RESULTS

A. *Flow visualization*

Figure 2 shows the flow of the carbon dioxide fog mixture through the circular hole and the shaped hole. Note the marked difference in the trajectory of the jet, although the mass flow rate through the holes is essentially the same. The jet from the shaped hole lies much closer to the surface through which it enters, while the jet from the cylindrical channel penetrates far from the wall. The fact that the jet leaving the shaped hole stays closer to the surface indicates that the film cooling performance of this geometry should be better, particularly at moderate and high blowing rates.

B. *Film cooling measurements*

Effect of channel geometry. The above reasoning is verified by the results presented in Fig. 3, which shows the film cooling effectiveness downstream of a single with M and then decreases. The performance at a blowing rate $M = 0{\cdot}5$ is nearly the same as for the cylindrical injection passage; but for all larger blowing hole, either cylindrical or shaped. Note that, for the cylindrical hole, the effectiveness is very low at blowing rates (M) greater than 0·5 at essentially all distances downstream. This agrees with previous studies which attributed low film cooling effectiveness to the increased penetration of the jet. In contrast, note that the effectiveness for the shaped channel is less dependent on the blowing rate. The effectiveness first increases somewhat rates, the film cooling effectiveness is considerably better with the shaped hole. In two-dimensional film cooling, at least at moderate blowing rate, the film cooling effectiveness increases with blowing rate due to the increased heat capacity of the injected fluid.

In addition to measuring the film cooling with a single injection hole, it is important to test the performance with injection through a row of holes across the span of the tunnel as might be encountered in actual applications. Figure 4 shows the film cooling effectiveness downstream of the center hole, for a row of eleven holes with three-diameter spacing. Figure 4 presents results for both cylindrical passages and

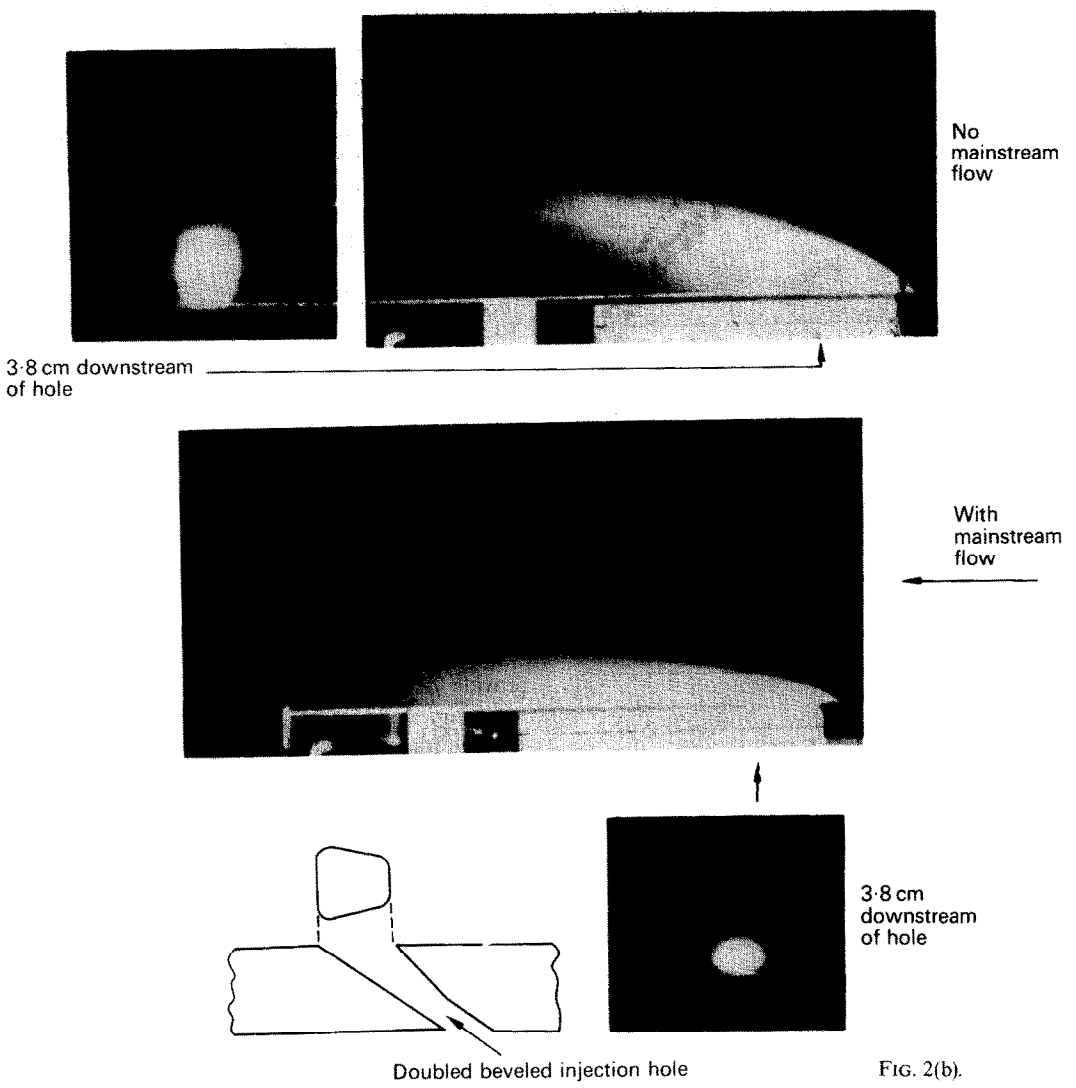

FIG. 2(b).

FIG. 2. Flow visualization study of jets leaving a cylindrical or shaped channel. (a) Jet from hole of constant circular cross section; (b) Jet from shaped hole (as in Fig. 1a).

shaped passages with the sides angled out by 10°. The results for cylindrical passages are similar to those obtained in previous studies (e.g. [1]). Some distance downstream of a row of cylindrical holes, the centerline effectiveness increases with increasing M apparently due to the coalescence of the jets.

With the shaped holes, the film cooling effectiveness at all blowing rates studied is considerably higher than with the cylindrical holes. With shaped holes, the effectiveness is essentially independent of M at small distances x/D and increases with M further downstream.

Figure 5 presents essentially the same data as Fig. 4 for the shaped holes, except that in this figure the centerline effectiveness is plotted against the parameter $X/(Ms)$, which has been used to correlate two-dimensional film cooling results. The lines on the figures are predictions [3] of the two-dimensional film cooling effectiveness for the range of injection Reynolds numbers studied. There is moderately good agreement with the prediction for all M values at values of the parameter $X/(Ms)$ larger than 100 and for the complete range of $X/(Ms)$ at $M \sim 0{\cdot}5$. Since the two-dimensional analysis primarily indicates the effects of a heat balance in the boundary layer when all of the secondary flow is spread across the span, the agreement would indicate that over the range of these tests the jets do not separate from the wall and essentially remain in the wall shear layer.

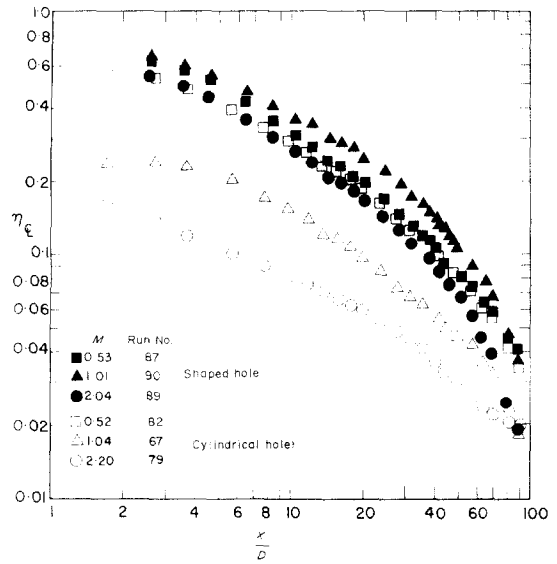

FIG. 3. Centerline effectiveness as a function of downstream position for different blowing rates of air injection through a single hole.

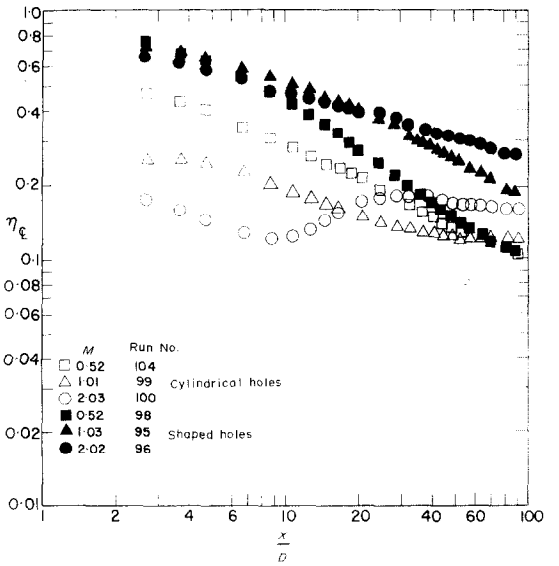

FIG. 4. Centerline effectiveness as a function of downstream position for injection of air through a row of 11 holes at three diameter spacing.

Table 1 gives parameters for the runs labeled in Figs. 3–5. Parameters for the following figures cover the same ranges.

A question arises as to what is the distribution of film cooling effectiveness across the span of the tunnel, i.e. how well the secondary fluid spreads laterally. Is there relatively good film cooling effectiveness only downstream of the center of the injection holes or do such jets spread further across the tunnel? One of the reasons for widening the channels sideways was to

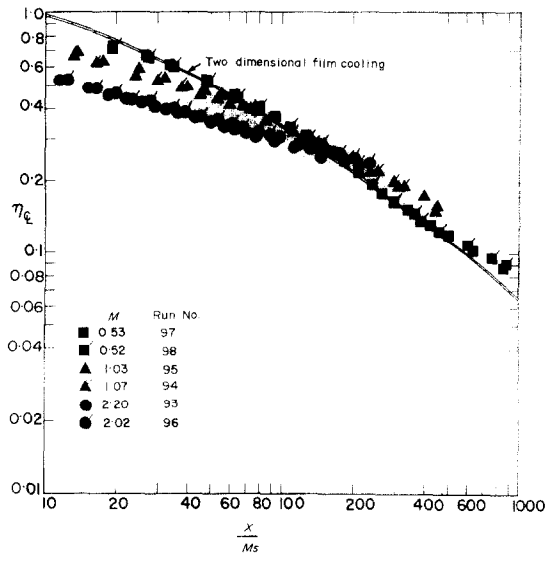

FIG. 5. Centerline effectiveness following injection of air through a row of shaped holes at 3 D spacing plotted against the parameter $X/(Ms)$.

provide for the possibility of greater spreading of the secondary flow across the tunnel wall. That this is essentially accomplished can be observed in comparing the data presented in Figs. 6a and 6b, which were obtained for conditions similar to those used in Fig. 4. Measurements of the effectiveness plotted in Fig. 6 are not obtained from the wall thermocouples, but rather from the rake of thermocouples which is pressed against the wall. This is done as there are too few thermocouples distributed across the span of the tunnel to determine lateral profiles of the effectiveness. Use of a rake pressed against the wall also has an advantage over measurements with thermocouples embedded in the wall in that it better approximates locally adiabatic wall conditions.

Table 1

Run No.	M	$Re_D \times 10^{-4}$	$\frac{\delta^*}{D}$
67	1·04	1·83	0·158
79	2·20	0·87	0·183
82	0·52	1·77	0·159
87	0·53	1·73	0·158
89	2·04	0·91	0·180
90	1·01	1·91	0·155
93	2·20	0·40	0·214
94	1·07	0·85	0·184
95	1·03	1·67	0·161
96	2·02	0·89	0·183
97	0·53	1·61	0·162
98	0·52	1·61	0·162
99	1·01	1·89	0·157
100	2·03	0·94	0·180
104	0·52	1·78	0·159

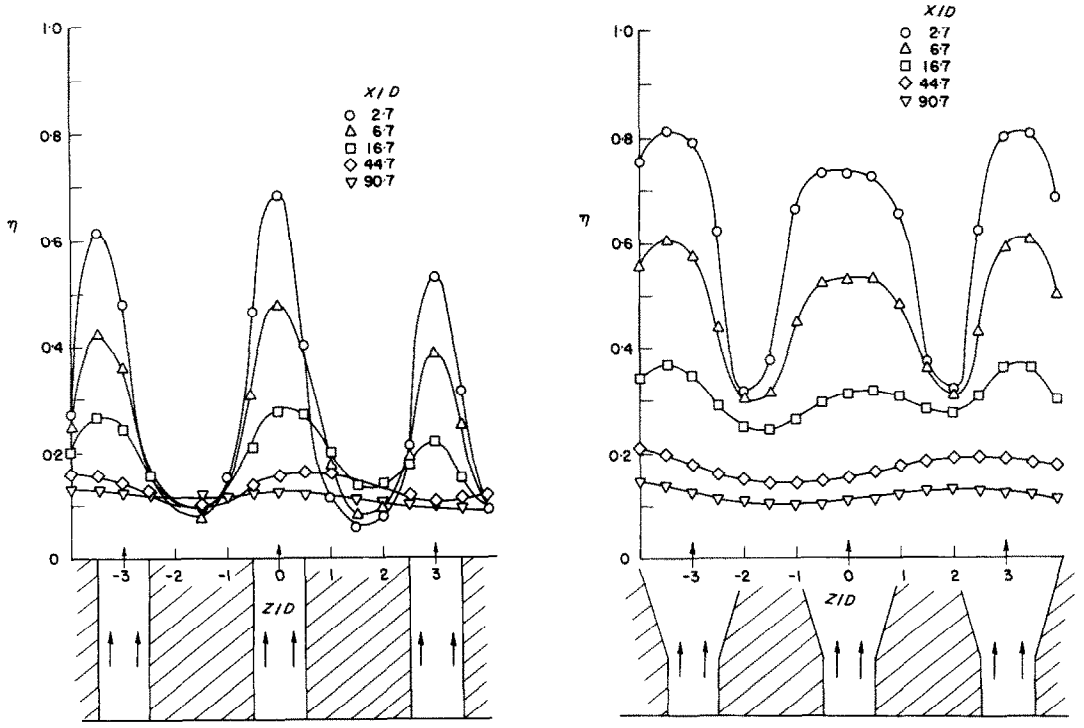

FIG. 6. Lateral variation of film cooling effectiveness with air injection through a row of holes with 3-diameter spacing for $M = 0{\cdot}5$. (a) Cylindrical holes; (b) Shaped holes.

The tunnel used was not specifically designed for three-dimensional studies and some conduction errors in the wall thermocouple measurements occurred, though a comparison with the rake measurements showed that the conduction errors were not too great. Figure 6a shows the effectiveness measured downstream of the three cylindrical injection channels in the center of the tunnel floor. Significant peaks downstream of the hole centerlines and valleys between holes are observed close to the injection location, while the lateral variations are smoothed out at large distances downstream. Figure 6b is a similar plot for the shaped hole injection section. A much broader temperature distribution is observed near the hole centerline where the effectiveness is high. Not only is the film cooling effectiveness directly downstream of a shaped hole higher than downstream of a round cylindrical hole, but relatively high effectiveness is maintained across an appreciable span between the positions of the injection hole, indicating that the mean effectiveness across the span has been improved with the shaped holes.

To determine how well the shaped holes would work with greater than $3D$ spacing, an injection section was made with holes spaced apart by six diameters. The results of rake measurements with this geometry are shown in Fig. 7. On this figure, the center of the tunnel ($Z/D = 0$) is halfway between two holes. Note

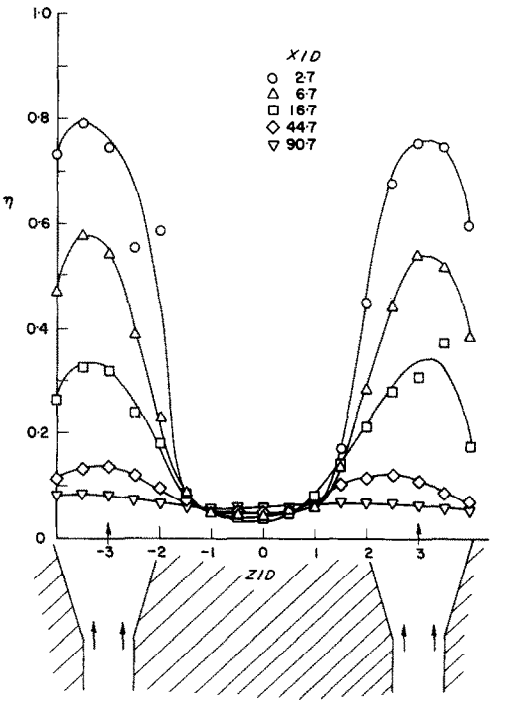

FIG. 7. Film cooling effectiveness as a function of lateral position for air injection through shaped holes spaced 6 diameters apart at $M = 0{\cdot}5$.

that the width of the film-cooled region downstream of the holes is not significantly greater than for $3D$ spacing, indicating that if such a wide spacing were used there would be large regions in between the holes which would not be directly protected by the film coolant.

Effect of blowing rate. A better understanding of the film-cooling phenomena can be obtained from cross plots of some of the data to show the influence of blowing rate. Figure 8 shows such curves of the centerline effectiveness at two different downstream positions. Note that the effectiveness values for the two geometries

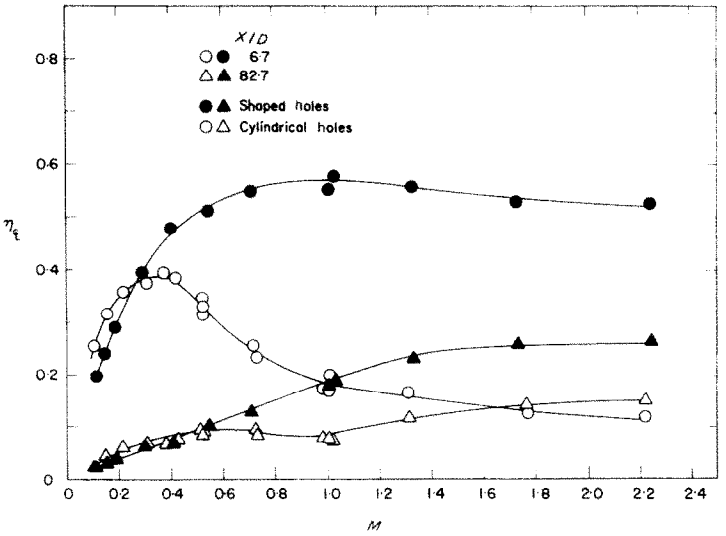

FIG. 8. Centerline effectiveness as a function of blowing rate for injection of air through straight round holes and shaped holes. Row of holes on $3D$ spacing.

are in reasonable agreement with each other at low M. The significant decline in film cooling effectiveness with increased blowing through cylindrical secondary flow channels has been attributed to the penetration of the secondary fluid jets into the mainstream away from the adiabatic surface. Figure 8 shows that, up to the blowing rate that produces separation from the wall, the two geometries give very similar results. For high blowing rates, a decline in effectiveness occurs with the shaped channel injection at the downstream position closest to the hole. This decrease is moderate and occurs only at a relatively high value of M.

Figure 9 shows the variation in film cooling effectiveness with blowing rate for two positions downstream of the cylindrical channels, both for a single hole and for a row of holes with a three-diameter spacing. Note that close to the hole there is not a great deal of difference between the results for a single hole and a row of holes. Further downstream there is a pronounced effect, particularly at large blowing rates, where with a row of holes the jets from the individual holes appear to coalesce and give better protection than the jet coming from a single hole.

It is important to be able to predict the blowing rate at which jet penetration into the mainstream becomes significant. With a shaped hole perhaps a quasi-blowing parameter or modified blowing parameter based on the actual exit area should be used. This would assume that the flow in the shaped channels fills the entire cross-section at exit, but otherwise behaves like the jet leaving the cylindrical channel. The ratio of the area of the exit hole to that at the entrance to the secondary flow passage (the metering hole area used to determine M) is denoted by the symbol, R. For the shaped holes described in these tests, R has the value of 2·55. For the cylindrical injection channels R is, of course, unity. The centerline effectiveness downstream of injection through a single shaped hole (used to get a large range of M) is plotted vs the ratio M/R in Fig. 10. A comparison with the dashed curves for the round hole and with Fig. 9 indicates that for the two different geometries, the maximum effectiveness is reached at about the same value of M/R. This lends credence to the assumption that jet penetration is determined by the "mean" mass velocity ratio of the secondary flow to the mainstream flow based on the exit area, at least when the secondary and mainstream fluids have almost the same density.

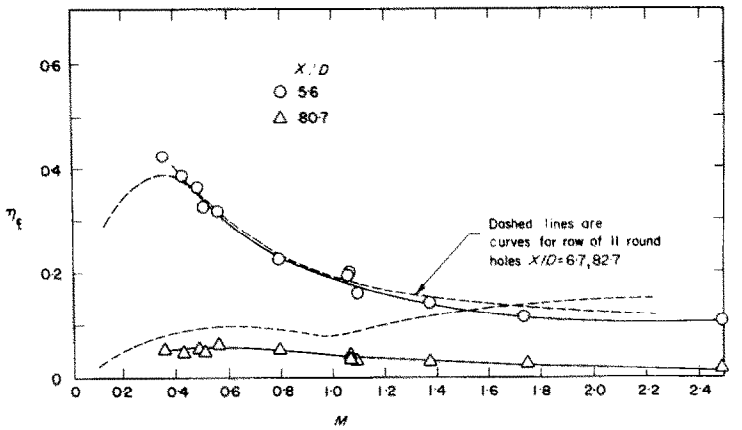

FIG. 9. Centerline effectiveness as a function of blowing rate for injection of air through a single cylindrical hole.

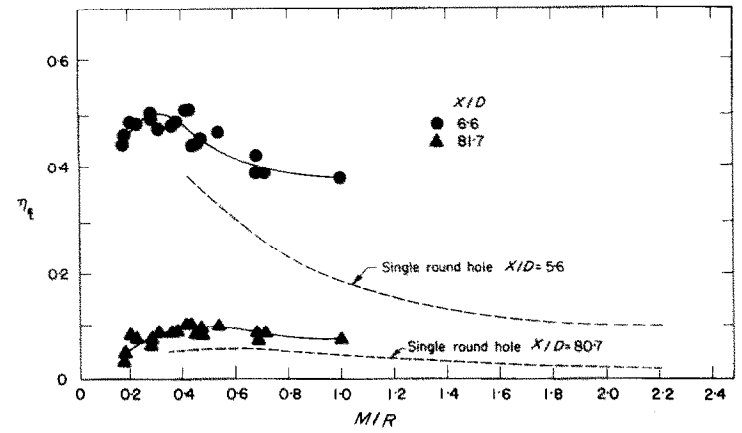

FIG. 10. Centerline effectiveness as a function of blowing rate divided by area ratio for air injection through a single shaped hole.

It should be borne in mind that if there are abrupt changes in the cross-section of the secondary flow channel, separation can occur within the channel and the above conclusion may not hold.

Effect of density ratio. In many actual applications, the density of the coolant is considerably higher than that of the primary flow, as the former is much cooler than the latter. In addition, a difference in density might be due to the different chemical nature of the two fluids. To determine the effect of the density variation on three-dimensional film cooling, some tests were performed using refrigerant-12 (Freon) vapor ($\rho_2/\rho_\infty \simeq 3{\cdot}5$) as the secondary fluid injected into the air mainstream. A single 6·35 mm diameter channel was used, either cylindrical or shaped (angled 10 degrees to each side as in Fig. 1a). Figure 11 shows the variation of the centerline film cooling effectiveness for refrigerant injection at two different downstream positions as a function of M/R. The use of the area ratio brings the data for both geometries together quite well. A comparison of Fig. 11 with Fig. 10 shows that the value of M/R at which the maximum effectiveness occurs is considerably larger for refrigerant injection than for air injection.

In Fig. 12 the film cooling effectiveness is plotted vs the ratio of the momentum flux of the entering jet to the momentum flux in the free stream ($I = \rho_2 U_2^2/\rho_\infty U_\infty^2$) for both air and refrigerant injection. The refrigerant results are all for single cylindrical hole injection; the air results are for both injection through a single cylindrical hole and through a row of cylindrical holes. Note that there is reasonable agreement in the (horizontal) positions of the maxima of the film cooling effectiveness plotted as a function of the momentum flux ratio. This is best seen by comparing the row of holes data for air versus the single hole data

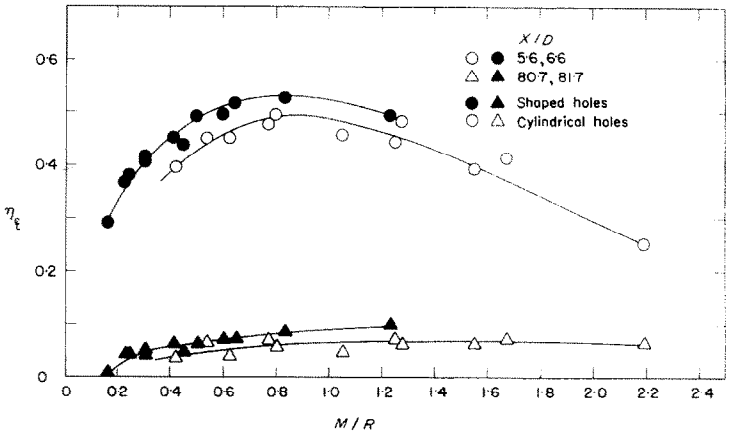

FIG. 11. Centerline effectiveness as a function of blowing rate divided by area ratio for refrigerant-12 injection through a single shaped hole and a single cylindrical hole.

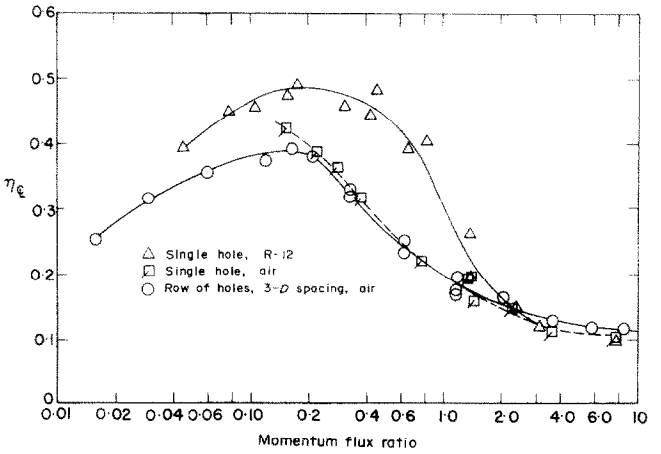

FIG. 12. Centerline effectiveness as a function of momentum flux ratio for refrigerant-12 and for air injection through cylindrical holes at $X/d = 5{\cdot}6$ and $6{\cdot}7$.

for Freon, as there were not sufficient data taken at low blowing rates for the injection of air through a single hole.

Figure 13 is a similar plot of the results for refrigerant and air flow through shaped holes. Here again, relatively good agreement is found between the positions of the maxima for the secondary flows of very different density. The relatively close agreement in the magnitudes of the film cooling effectiveness for different injection fluids in both Figs. 12 and 13 may be fortuitous. A comparison of Fig. 12 with Fig. 13 indicates what might be a more general correlation which takes into account the effect of the shape of the secondary flow channel, at least in terms of determining the position of the maximum. For this purpose, attention is directed to the upper abscissa scale in Fig. 13. The parameter correlating film cooling effectiveness appears to be the momentum ratio divided by the area ratio squared. The parameter I/R^2 is, of course, the momentum flux ratio at the exit of the hole, assuming that the secondary flow completely fills the channel. The maximum film cooling effectiveness in Fig. 13 occurs at a value of I/R^2 of about 0·2, which is in relatively good agreement with the value shown on Fig. 12 (in which R is unity and $I = I/R^2$).

Effect of boundary layer thickness. Another parameter that affects film cooling performance is the ratio of the boundary layer thickness to the injection hole diameter.

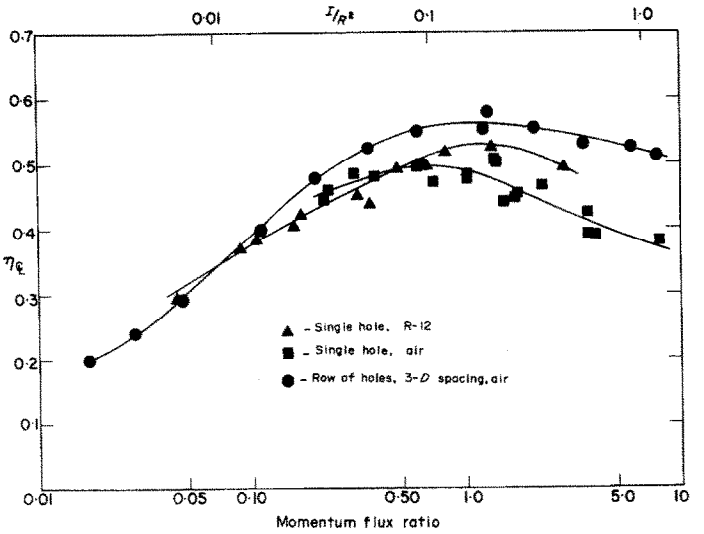

FIG. 13. Centerline effectiveness as a function of momentum flux ratio and momentum flux ratio modified by channel area for injection of refrigerant-12 and air through shaped holes at $X/d \sim 6{\cdot}7$.

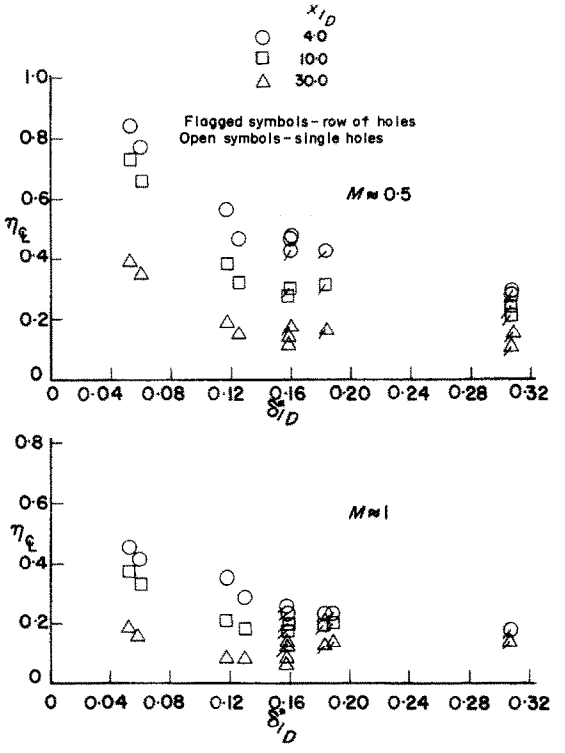

FIG. 14. Effect of upstream boundary layer thickness on centerline film cooling effectiveness for air injection through cylindrical holes.

Figure 14 shows the results of tests performed in the present study as well as those from [1]. Note that the trends reported earlier seem to be corroberated. The film cooling effectiveness decreases when the ratio of boundary layer thickness to injection hole diameter increases, although the trend is diminished at large δ^*/D. This decreased effectiveness has been attributed to the lower velocity mainstream fluid near the wall in a boundary layer which permits greater penetration of the jet. Note that some of the results are for injection through a row of holes. At large distances downstream there should be a greater difference between the results for a single hole and a row of holes due to merging of the jets from the row of holes.

IV. SUMMARY AND CONCLUSIONS

Experiments indicate the improvement of three-dimensional film cooling which can be obtained with shaped channels for the secondary flow. The use of a passage with an initially round cross section widened to each side by an angle of about 10 degrees significantly increases the film cooling effectiveness immediately downstream of either a single hole or a hole in a row of holes. In addition, the shaped hole appreciably increases the spreading of the secondary flow so that the film cooling effectiveness at positions laterally displaced from the centerline of a hole is also much greater than that found downstream of a cylindrical hole. One explanation of the increased effectiveness with shaped holes is that the mean velocity of the secondary flow is decreased with the larger exit area. This lower effective blowing rate causes the jet to stay closer to the wall rather than penetrating into the mainstream and accounts for the higher film cooling effectiveness, particularly at high blowing rates.

The use of refrigerant-12 as a secondary fluid gives an appreciably higher film cooling effectiveness at larger blowing rates than when air is injected. In particular, the maximum on an effectiveness vs blowing rate curve is at much larger values of blowing rate for refrigerant injection than for air injection.

The blowing rates at which maximum film cooling effectiveness is observed for the two geometries and two cooling fluids could be correlated by introducing the exit to entrance area ratio of the channel and by considering that not the mass velocity ratio but the momentum ratio or dynamic pressure ratio is the key parameter in determining penetration of the jet for fluids of different density.

Acknowledgement — This work was supported by the Aircraft Engine Division of the General Electric Co. at Evandale, Ohio. Significant contributions to the study were made by J. W. Ramsey, D. J. Wilson, V. E. Erikson, and T. Y. Chu. R. Rask helped in the preparation of the manuscript.

REFERENCES

1. R. J. Goldstein, E. R. G. Eckert, V. L. Eriksen and J. W. Ramsey, Film cooling following injection through inclined circular tubes, *Israel J. Technol.* **8**(1–2), 145 (1970).
2. G. N. Abramovich, *The Theory of Turbulent Jets*, pp. 541–556. M.I.T. Press, Massachusetts Institute of Technology, Cambridge, Massachusetts (1963).
3. R. J. Goldstein and A. Haji-Sheikh, Prediction of film cooling effectiveness, *Proceedings of Japanese Society of Mechanical Engineers*, Semi-International Symposium, Vol. 2, p. 213 (1967).

EFFETS DE LA GEOMETRIE D'ORIFICE ET DE LA DENSITE SUR LE REFROIDISSEMENT PAR FILM TRIDIMENSIONNEL

Résumé — On a étudié expérimentalement le refroidissement par injection d'un film de gaz secondaire à travers des orifices discrets. On décrit les influences de la géométrie du trou, de la densité du fluide secondaire et de l'épaisseur de la couche limite de l'écoulement principal. On a observé des accroissements significatifs de l'efficacité du refroidissement du film avec des canaux élargis avant la sortie du film secondaire. L'utilisation d'un fluide secondaire relativement dense, comme on pourrait le rencontrer dans de nombreuses applications, demande pour provoquer la séparation du jet de la surface un débit de soufflage nettement plus grand que lorsque les densités du courant libre et du courant secondaire sont égales. Il résulte de cette étude un refroidissement par film considérablement amélioré pour un domaine important de rapports de densité.

EFFEKTE DER LOCHGEOMETRIE UND DER DICHTE BEI DREIDIMENSIONALER FILMKÜHLUNG

Zusammenfassung — Filmkühlung nach Sekundärgasinjektion durch Einzelbohrungen wurde experimentell untersucht.

Die Einflüsse der Lochgeometrie, der Sekundärfluiddichte und der Grenzschichtdicke des Hauptstrahles werden beschrieben. Man beobachtet eine Verbesserung der Filmkühlwirkung, wenn man die Durchgänge für das Kühlfluid vor dem Austritt des Sekundärfluides erweitert. Die Verwendung eines relativ dichten Sekundärfluides, wie es bei vielen Anwendungen vorkommt, erfordert ein bedeutend stärkeres Gebläse, um eine Trennung des Strahls von der Oberfläche zu erreichen, als bei Dichtegleichheit des Freistrahls und des Sekundärstrahles. Daraus ergibt sich über einen wichtigen Bereich der Dichteverhältnisse eine wesentlich bessere Filmkühlung.

ВЛИЯНИЕ ГЕОМЕТРИИ ОТВЕРСТИЯ И ПЛОТНОСТИ ЖИДКОСТИ НА ТРЁХМЕРНОЕ ПЛЁНОЧНОЕ ОХЛАЖДЕНИЕ

Аннотация — Экспериментально исследовался процесс пленочного охлаждения вниз по потоку от места вдува вторичного газа через дискретные отверстия. Описывается влияние на этот процесс геометрии отверстия, плотности вторичной жидкости и толщины пограничного слоя основного потока. Значительное увеличение эффективности пленочного охлаждения наблюдалось в случае, когда подводящие охладитель каналы расширялись к месту выхода вторичной жидкости. Использование вторичной жидкости относительно более высокой плотности (что часто встречается на практике) требует значительно более высоких скоростей вдува для оттеснения потока от поверхности по сравнению со случаем, когда плотности основного и вторичного потоков одинаковы. В результате достигается значительное повышение эффективности пленочного охлаждения в диапазоне безразмерной плотности, имеющем важное практическое значение.